Science of Advanced Materials
Vol. 4, pp. 455–462, 2012
(www.aspbs.com/sam)

Pressure-Induced Growth Evolution of Different ZnO Nanostructures by a Pulsed Laser Ablation Method

P. Zhang[1], G. D. Zhou[1], H. B. Gong[1], H. Y. Xu[1], D. Nakamura[2], T. Okada[2], H. B. Zeng[3,*], and B. Q. Cao[1,*]

[1] *School of Physics, School of Materials Science and Engineering, University of Jinan, Jinan, 250022, Shandong, China*
[2] *Graduate School of Information Science and Electrical Engineering, Kyushu University, Fukuoka, 819-0395, Japan*
[3] *State Key Laboratory of Mechanics and Control of Mechanical Structures, Key Laboratory for Intelligent Nano Materials and Devices of the Ministry of Education, and College of Material Science and Technology, Nanjing University of Aeronautics and Astronautics, Nanjing 210016, China*

ABSTRACT

ZnO nanostructure growth evolution from well-aligned two-dimensional nanowalls to one-dimensional nanowire arrays and finally to zero-dimensional nanoparticles was successfully demonstrated by a pulsed laser ablation and deposition growth method, where the growth pressure was proved to be the determinant factor for the formation of different ZnO nanostructures. At lower pressure, nanowall grew due to a prefer nucleation at the grain boundary of a ZnO wetting layer via a vapor–solid process. At middle growth pressure, the ZnO nanowire growth can be described with a nanoparticle-assisted pulsed laser deposition process. At higher growth pressure, due to the strong collision between the ablated ZnO clusters and background gas, only nanoparticles were deposited. These ZnO nanostructured arrays had a preferred c-axis growth orientation on c-cut sapphire substrates. The photoluminescence and field emission properties were also studied.

KEYWORDS: High-Pressure PLD, Nanowall, Nanowire, ZnO, Field Emission.

1. INTRODUCTION

Nanomaterials such as one-dimensional (1D) nanowires and two-dimensional (2D) nanoplates, nanowalls, and graphen are receiving significant attention for applications in novel nanoelectronic and optoelectronic devices due to their unique structures and novel optoelectronic properties.[1,2] In this regard, zinc oxide (ZnO), with a direct band gap of 3.37 eV and a high exciton binding energy of 60 meV at room temperature, is an important II–VI compound oxide semiconductor which has great applications in light emitting diodes and transistor devices.[3,4] It manifests its properties especially when approaching the nanoscale size, for example, in the form of 1D nanowires[5] or 2D nanosheets,[6] which have been widely accepted as the building blocks for nanodevices. In view of this point, rational growth of nanostructures in terms of size, shape, and orientation is a prerequisite, and a large amount of intensive researches have been conducted to grow desired ZnO architectures. Typically, 1D ZnO nanomaterials are grown with a physical/chemical vapor evaporation and deposition method on a substrate with metal catalyst which produces a vertical array of nanowires with *c*-orientation. Until now, a variety of one-dimensional nanostructures like nanowires, nanobelts, nanorings, and other hierarchical nanostructures have been grown through this strategy and used to construct functional devices.[7,8] Moreover, few of them were also reported to synthesis 2D ZnO nanosheets/nanowalls.[9,10]

Pulsed laser deposition (PLD) is a typical vapor-phase growth method by condensation of a laser plume ablated from a pressed target, excited by the high-energy laser pulses far from equilibrium and usually adopted for thin films growth with excellent physical properties.[11] For example, high-quality ZnO films can heteroepitaxy on GaN sapphire and even silicon substrates.[12] Pulsed laser ablation (PLA) in a flowing vapor phase can also be adopted to grow nanowires. Lieber et al.[13] first used laser ablation to synthesized silicon and germanium nanowires through the traditional vapor–liquid–solid (VLS) mechanism with iron as catalyst. Few reports of ZnO nanorods synthesis by PLD methods in a quasi-static vapor environment have appeared thus far. For example, Yan et al.[14]

---

*Authors to whom correspondence should be addressed.
Emails: mse_caobq@ujn.edu.cn, zeng.haibo.nano@gmail.com
Received: 18 April 2011
Accepted: 11 May 2011

demonstrated growth of oriented Ga-doped ZnO nanorods arrays on GaN/sapphire substrates, but only at certain specific Ga-doping levels. Lorenz et al.[15] have reported growth of ZnO nanowires on sapphire in the presence of gold colloid catalysts. Cao et al.[16] reported the growth 2D ZnO nanowall arrays by high-pressure PLD through target doping in a straight quartz tube But, due to their structural polarity of hexagonal wurtzite ZnO, the rational synthesis of ZnO nanostructures with different dimensionalities is still challenging no mater what growth methods were applied. In this paper, we reported the growth evolution of ZnO from nanowall to nanowire with pressure by a new-designed high-pressure pulsed laser ablation and deposition system with a cross quartz tube and their photoluminescence (PL) and field emission (FE) properties.

2. EXPERIMENTAL DETAILS

A new designed and home-built high-pressure pulsed laser ablation and deposition system was schematically illustrated in Figure 1. A temperature-controlled electrical furnace with a cross-shaped quartz tube was used as the ablation and deposition chamber. The carrier and reaction gasses were monitored with different mass flow controllers (D07-19B, SevenStars, Beijing). The pressure were pumped with a mechanical pump and maintained with a MSK pressure/flow control module (250E, 248A and 626B). The targets were fixed at the cross-sectional part of the tube and can be rotate automatically. KrF excimer laser (Compex250, Coherent) were used to ablate ZnO targets, which were prepared with a standard powder chemical route by ball milling ZnO powders, cold pressing and subsequent sintering at 1100 °C for 5 h in air. Sapphire was used as substrate without any catalyst The distance between the substrate and ZnO target was 15 mm. The growth temperature was 900 °C and argon was used as carrier gas with a flux of 50 SCCM.

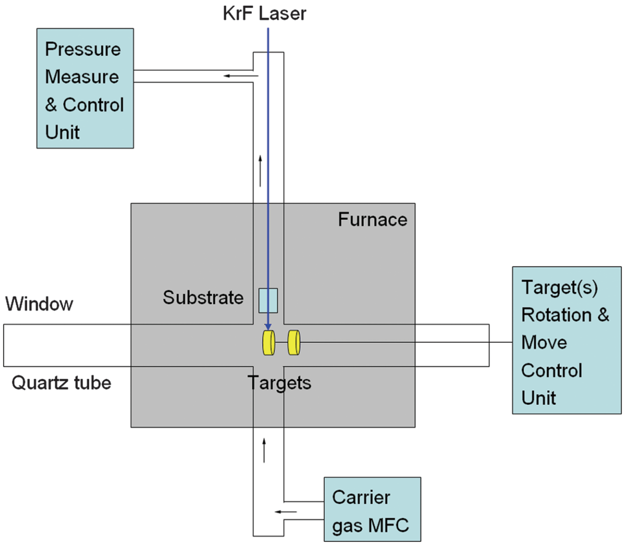

Fig. 1. A schematic illustration of the home-built PLA growth system used for ZnO nanostructure growth.

The sample morphologies were observed with a field-emission scanning electron microscopy (SEM, Quanta, FEI) and powder X-ray diffraction (XRD) measurements using an X-ray diffractometer (D8-ADVANCE, Bruker) with Bragg–Brentano geometry using $\mathrm{Cu}_{K\alpha}$ radiation. Transmission electron microscope (TEM, JEM-2010, JEOL) was used to observe the microstructure of the prepared samples. The photoluminescence (PL) spectra of ZnO nanostructures were measured with a home-built PL spectrometer excited with Xenon lamp (500 W, Osram). The field-emission properties of the different samples were studied at room temperature in a high vacuum chamber (10^{-6} Pa) using a 1 mm^2 cross-sectional area aluminum anode. A dcvoltage sweeping from 100 to 1100 V was applied to a sample at a step of 50 V. The electrical current was measured with a Keithley 2400 source/meter.

3. RESULTS AND DISCUSSION

3.1. ZnO Nanostructures Characterizations and Growth Evolution

Figure 2 shows the morphology evolutions of the ZnO samples with the PLA growth pressure from 10 Torr to 175 Torr. Typically, when the background growth pressure was set at 20 Torr, the synthesized sample showed very little resemblance to the planar ZnO films. They are well-aligned ZnO nanowalls with a thickness of tens of nanometers and dimension of several micrometers. Figure 2(a) shows typical SEM images of the ZnO nanowalls grown on sapphire substrates in 45 minutes. Most of the nanowalls were perpendicular to the substrate and formed an interconnected nanowall network simultaneously as shown in Figure 2(b). With the growth pressure further increasing, the interconnected nanowalls broke and mixture of longer nanobelts and nanowires were grown, as shown in Figures 2(c, d), where the pressure was maintained at 70 Torr. Finally, when the pressure is higher than 120 Torr, 1D ZnO nanowire array grew on the sapphire substrate, which is similar to the former report of Lorenz.[15] When the background pressure was further increased, only aggregation of big ZnO nanoparticles was obtained, as typically shown in Figures 1(g) and (h) for 150 Torr and 175 Torr, respectively.

The phase and orientation of the PLA grown ZnO nanowalls was studied with XRD measurements. Figure 3 shows the XRD 2θ diffraction patterns of the samples in Figure 2. For the nanostructural array samples, only two groups of strong diffraction peaks were observed. The peaks at 41.8 degree are due to the sapphire substrate (006)-peak diffraction. Another group of peaks at 34.6 degree is the (002)-peak diffraction of hexagonal

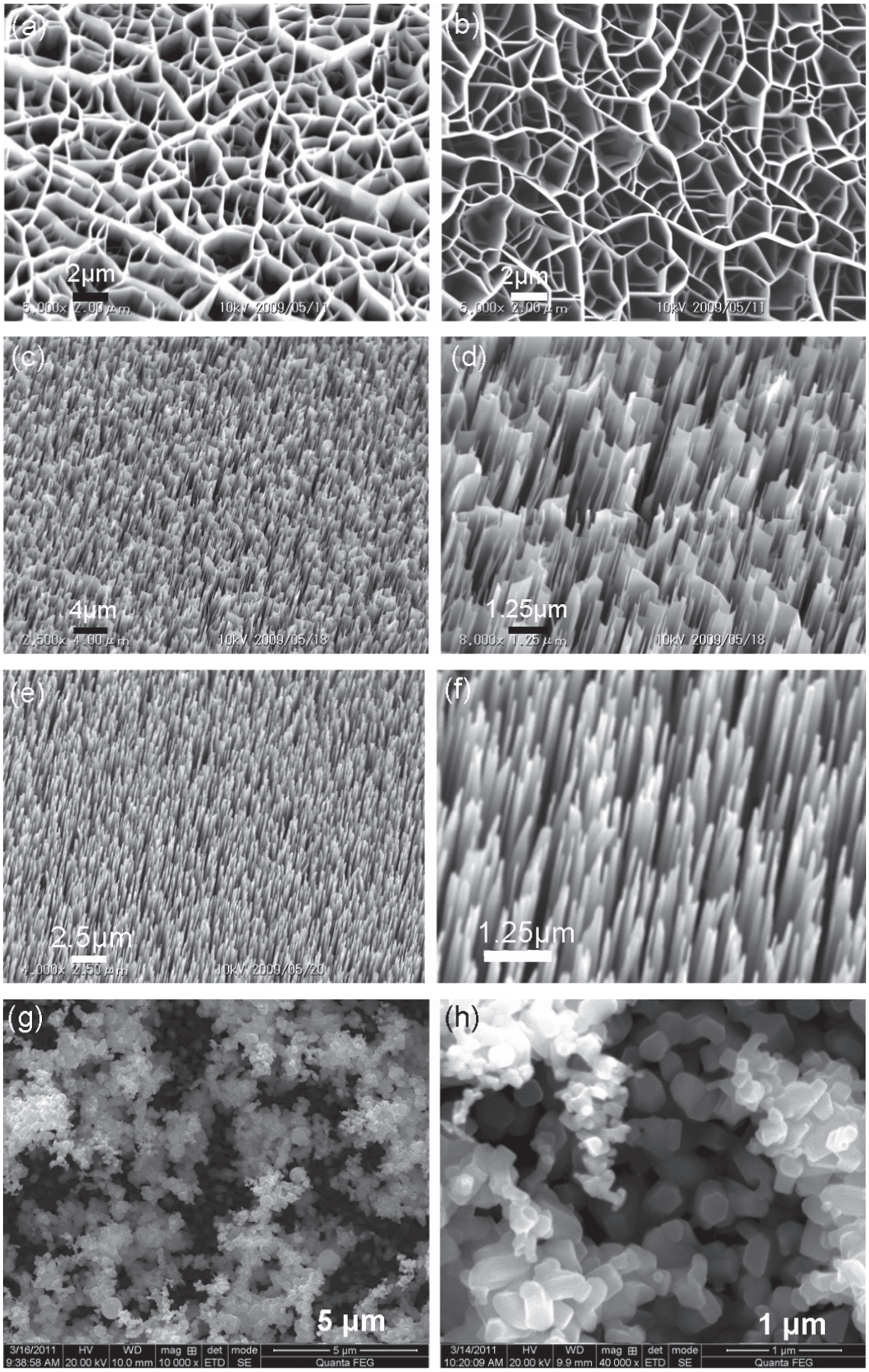

Fig. 2. SEM images of the different ZnO nanostructures grown with a PLA method under different pressure. (a, b) Nanowall interconnected network (20 Torr); (c, d) Mixture of nanowall and nanowire (70 Torr); (e, f) Nanowire array (140 Torr); (g, h) Nanoparticles (150 and 175 Torr).

wurtzite phase of ZnO. Therefore, the XRD result indicated clearly that the PLA grown ZnO nanowalls and nanowires show obvious preferred *c*-orientation and a good epitaxial relation between the *c*-planes of ZnO and sapphire substrate. But, due to the structure inhomogeneity, the full width at half maximum (FWHM, ~0.5 degree) of ZnO nanowire/nanowall mixture is bigger than that (~0.2 degree) of pure nanowires or nanowalls. The XRD

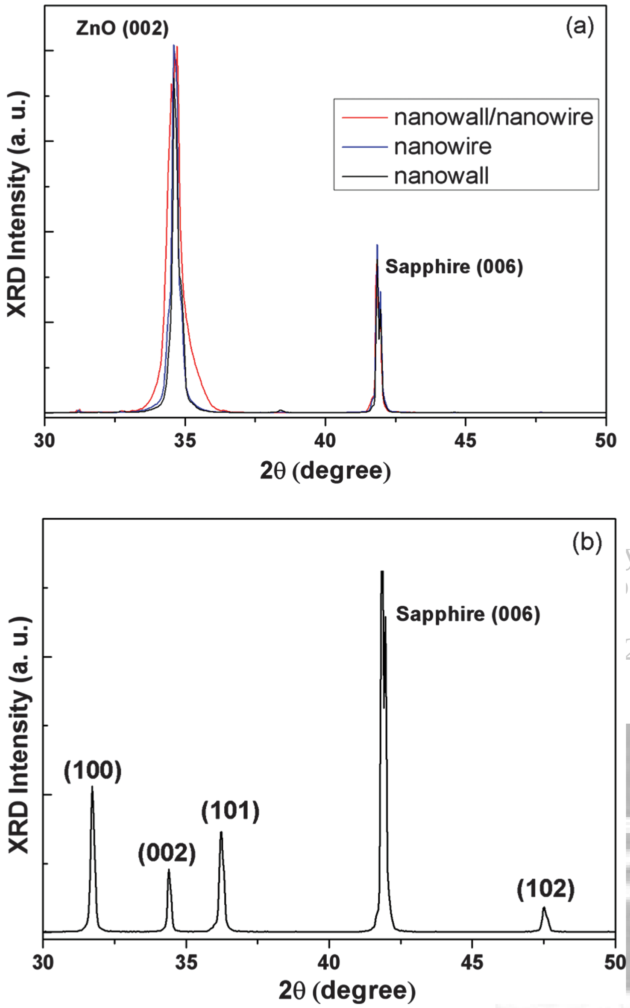

Fig. 3. (a) XRD spectra of different ZnO nanostructural arrays grown on sapphire substrates, (b) XRD spectrum of ZnO nanoparticles grown on sapphire substrate.

spectrum of nanoparticle sample exhibited all the typical diffraction peaks from wurtzite ZnO (JCPDS 36–1451), as shown in Figure 3(b).

Further microstructural characterizations were performed with TEM. The ZnO nanowall or nanowire samples were first scratched from the substrates and then transferred onto a copper grid meshes for TEM observations. Figures 4(a) and (b) show a low-magnification TEM image of a ZnO wall flake and its corresponding high-resolution TEM image. This nanowall flake has an irregular triangular shape with a length of few micrometers, which was possibly caused by the scratching process for TEM sample preparation. The brightness difference of the flake between the top and the bottom parts indicated that the nanowall flake is curled, as typically shown in the SEM image of Figure 2(b). The high-resolution TEM image of Figure 4(b) shows that the ZnO nanowall flake has single crystal structure and the lattice spacing of 0.26 nm corresponds to the d spacing of (001) crystal planes of ZnO. Figure 4(c) is the TEM image of a single ZnO nanowire. HRTEM examination has indicated that the ZnO nanowire is of single-crystal structure without visible defects, as shown in Figure 4(d). This HRTEM image clearly shows the (0001) crystal planes perpendicular to the axis of the nanowire, indicating that $\langle 0001 \rangle$ is the preferred growth direction of the wurtzite nanowire. Both the TEM results of ZnO nanowall and nanowire further confirmed the XRD analysis that they were both preferentially oriented in (001)-direction.

It is clearly illustrated here that the growth of different ZnO nanostructures with PLA was mainly determined by the growth pressure as no catalyst was used in the experiment. To study the growth mechanism, the growth process of ZnO nanowalls was first investigated with SEM for the different growth period, as shown in Figure 5. Based on the obtained experimental results, a vapor–solid (VS) process was proposed for ZnO nanowalls. When the ablated source materials were deposited on the substrate under a growth pressure of 20 Torr which was much higher than that for film growth, typically 10^{-3} Torr, a network of ZnO thin layer with narrow grain boundaries could first form on the substrate in the first ten minutes, as shown in Figure 5(a). Then, ZnO nucleations could preferably take place at the grain boundary via the VS mechanism (Fig. 5(b)), as grain boundaries provide low surface energy for nucleation.[17] It is well known that ZnO is a kind of polar crystal and the polar plane $\{0001\}$ has higher surface energy than the other two non-polar surfaces, $\{2\bar{1}\bar{1}0\}$ and $\{01\bar{1}0\}$. So fast crystal growth along the $\langle 0001 \rangle$ direction is energetically favorable under thermodynamical equilibrium conditions Finally, interconnected 2D nanowalls network formed when these grains continued to grow, as illustrated with Figures 5(c) and (d).

With the growth pressure increasing, the abruption of interconnected nanowall network was observed due to the fast growth along the c-axis and, therefore, a nanowall and nanowire mixture was observed at a growth pressure of 70 Torr. Pure ZnO nanowire array was obtained at 140 Torr. Obviously, the growth mechanism of ZnO nanowires with PLA is not the traditional vapor–liquid–solid (VLS) process, as no extrinsic metal catalysts were used here. To disclose the growth process of the nanowires, Guo et al.[18] studied the initial growth stage of the nanowires synthesized by high pressure PLA method. After 10 min laser ablation, ZnO nanoparticles with average diameter of 100 nm were deposited on the sapphire substrate at the initial growth stage. These nanoparticles were formed in the gas phase due to the high background pressure, as observed with Rayleigh scattering.[19] When the particles were transported onto the substrate at high temperature, they melted and migrated on the substrate. During this process, the nanoparticles aggregated each other. As a result of the melting temperature getting higher with the size of aggregated particles, they precipitated at some

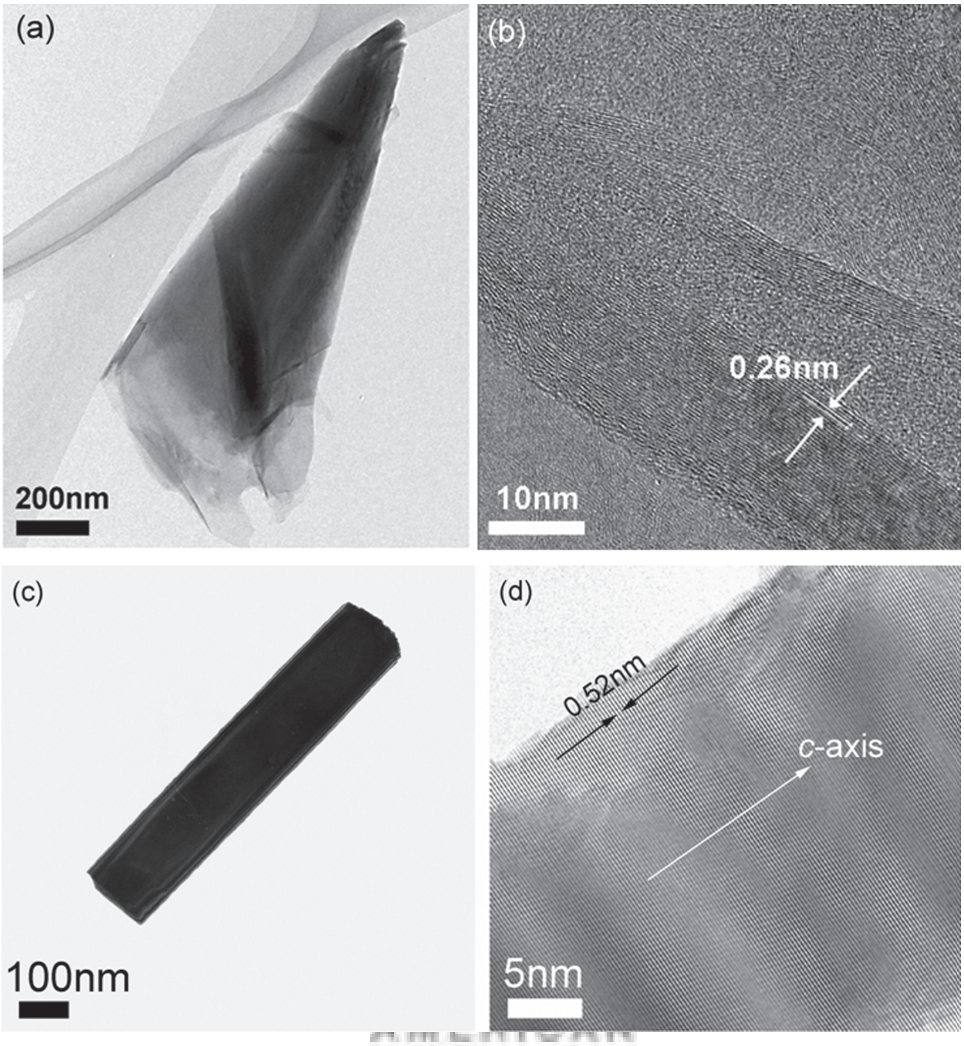

Fig. 4. (a) Low-magnification TEM image of a piece of ZnO nanowall and (b) its HRTEM image taken from the bottom edge part of the nanowall. (c) Low-magnification TEM image of a ZnO nanowire and (d) its HRTEM image.

places on the substrate. The isolated nanocrystals could serve as nucleation centers to initiate the growth of ZnO nanowires. Therefore, such nanowires grown with high-pressure PLA usually with bigger nanoparticles as roots and thinner nanowire as stems was called as nanoparticle-assisted pulsed laser deposition (NAPLD),[20] which was significantly different from that of the metal catalyzed vapor–solid–liquid growth process previously reported.[21] When the growth pressure was further increased, the strong collision of ZnO ablated clusters only led to the formation of nanoparticles randomly deposited on the substrate, as shown in Figures 2(g) and (h).

3.2. Photoluminescence and Field Emission Properties of ZnO Nanowires and Nanowalls

The optical properties of the different ZnO nanostructures were studied by PL spectrum excited with 325 nm light from a xenon lamp at room temperature, as shown in Figure 6. A dominant near band-edge (NBG) emission peak centered at about 380 nm with an FWHM of 110 meV was observed for all samples, which originated from the recombination of free or bound excitons. Except ZnO nanowires, typical green emission peaks centered at around 520 nm in the room-temperature PL spectra were also observed, in addition to the UV emission peak. This emission was generally attributed to the deep-level defects in ZnO crystals, such as vacancies and interstitials of zinc or oxygen in the surface layer.[22, 23] In this work, the green emission of ZnO nanowire was so weak that it can be negligible. The strong and sharp UV emission and the weak green emission indicated that the ZnO nanowires were of better crystal quality than ZnO nanowalls. The possible reason was that a well-crystallized surface was formed during the free standing nanowire growth process as shown in the HRTEM image (Fig. 4(d)), where no visible defect or amorphous layer was observed.

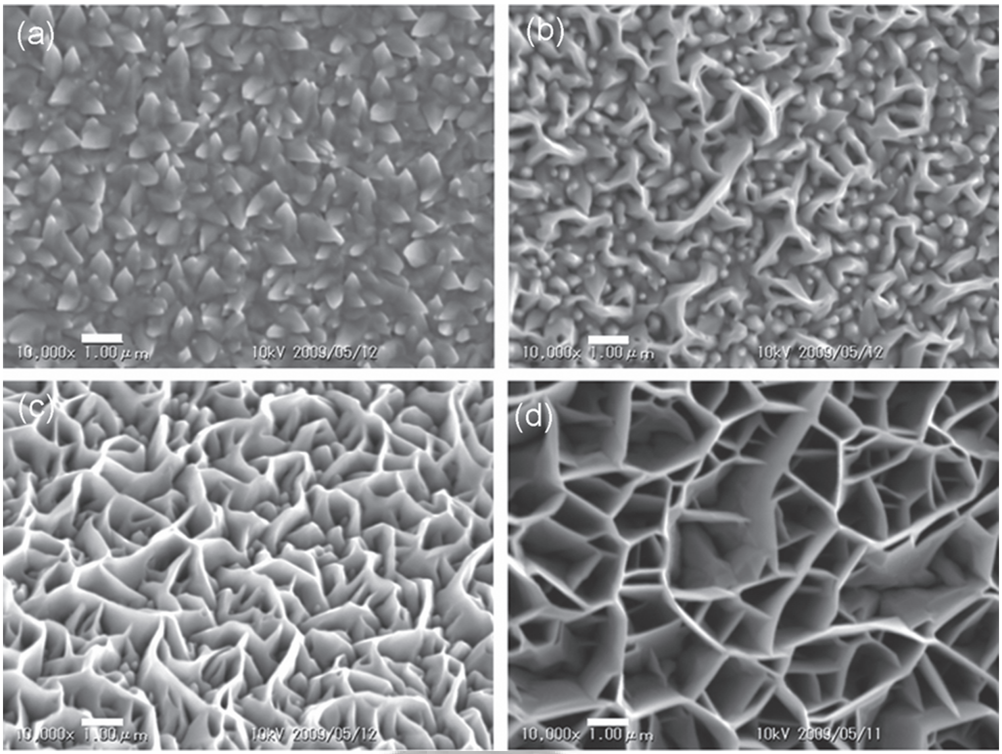

Fig. 5. ZnO nanowalls growth process at different time observed with SEM (a) 10 min, (b) 15 min, (c) 25 min, and (d) 45 min.

The field emission properties of such ZnO nanowall and nanowall and nanowire mixture samples were measured in a vacuum chamber at room temperature by depositing two parallel gold contacts. But the isolated ZnO nanowire sample on sapphire substrate was not conductive enough for field emission measurement. Figure 7(a) shows the current density versus applied electrical field (J-E) curves of ZnO nanowall and nanowall/nanowire mixture. The turn-on field, defined as the applied field to draw an emission current of 1 μA/cm^2, is about 15 and 22.5 V/μm, respectively, lower than the turn-on value (18 V/μm for 0.01 μA/cm^2) of ZnO needles grown on gallium-doped ZnO film by vapor phase method.[24] Our value is comparable to that of the silicon nanocone arrays prepared by ion sputtering.[25]

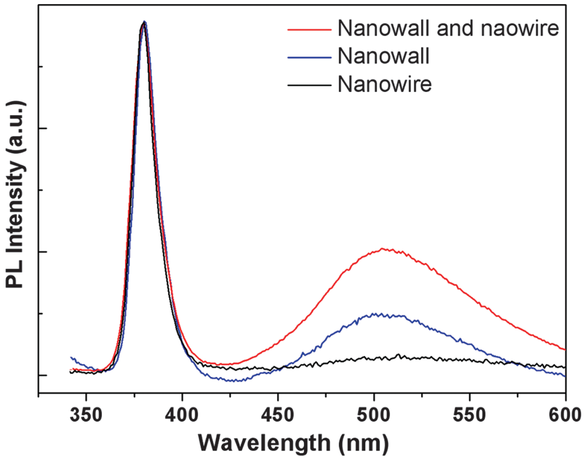

Fig. 6. Normalized room-temperature PL spectra measured from three samples shown in Figure 2.

According to the Fowler-Nordheim (F-N) theory, the relationship between current density (J) and applied electric field (E) can be described as follows,[26]

$$J = A\left(\frac{\beta^2 E^2}{\Phi}\right)\exp\left(\frac{-B\Phi^{3/2}}{\beta E}\right) \tag{1}$$

where $A = 1.54 \times 10^{-10}$ (AV^{-2} eV), $B = 6.83 \times 10^9$ (Vm^{-1} eV$^{-3/2}$), and Φ is the work function, which is about 5.4 eV for ZnO. And β is the field enhancement factor defined as: $E_{\text{local}} = \beta E = \beta V/d$, where E_{local} is the local electric field nearby the emitter tip. According to F-N theory, the plot of $Ln(J/E^2)$ Vs E^{-1} (F-N plot) should be a straight line. From data in Figure 7(a), corresponding F-N plots were shown in Figure 7(b). All the F-N plots show nearly straight-lines with slightly different slopes, indicating the field emission process was a barrier tunneling, quantum mechanical process (F-N mechanism). The slopes obtained from the F-N plots can be used to estimate the β values, as shown in Figure 7(b), which were better than the reported values of ZnO nanotips (657 at $d = 250$ μm)[27] or multi-wall carbon nanowires (830 at $d = 125$ μm).[28] As the one-dimensional semiconductor nanowires have smaller radius of curvature, which enhances their field emission properties, the field emission properties of nanowire/nanowall mixture sample was better

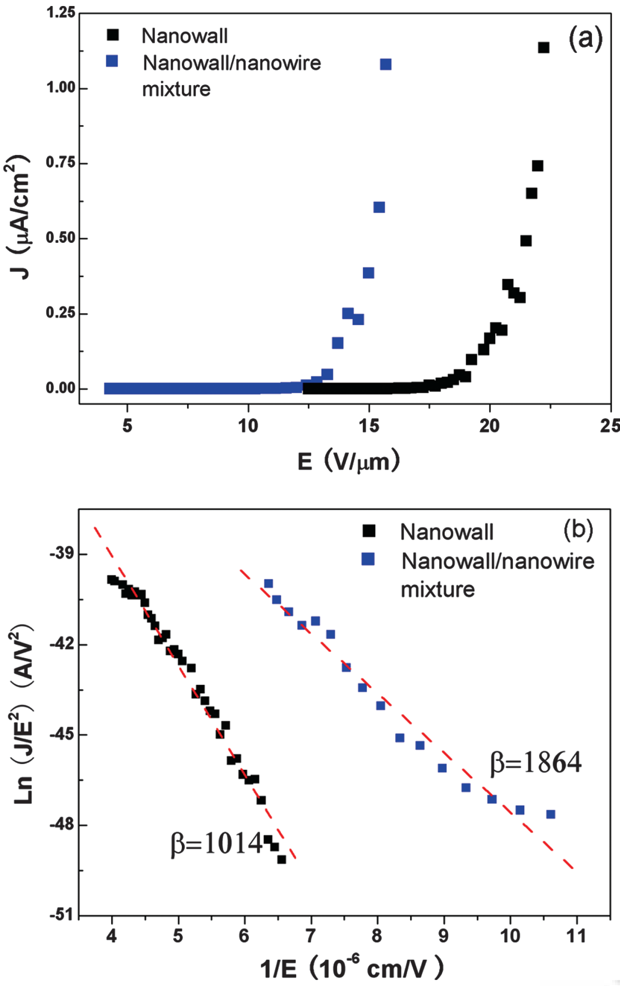

Fig. 7. (a) Field emission curves ($J \sim E$) of the ZnO nanowall and nanowall/nanowire mixture samples and (b) the corresponding F-N plots [$\ln(J/E^2) \sim 1/E$] from panel (a).

than that of pure ZnO nanowall in terms of turn-on electrical field and field enhancement factor.[29] So, it can also be expected that the nanowire arrays would show much better field emission performance if they could be grown on a conductive substrate which is needed for practical field emission display applications.

4. CONCLUSION

In summary, ZnO nanostructure growth evolution from well-aligned 2D nanowalls to 1D nanowire arrays and finally to 0D nanoparticles was successfully demonstrated by a high-pressure pulsed laser ablation and deposition growth method, where the growth pressure was proved to be the determinant factor for the formation of different ZnO nanostructures. At rather low pressure of 20 Torr, the ZnO nanowall growth was due to a prefer nucleation at the grain boundary of a ZnO wetting layer via the VS mechanism, as grain boundaries provide low surface energy for nucleation. At middle growth pressure, the ZnO nanowire growth can be described with the typical nanoparticle-assisted pulsed laser deposition process. If growth pressure was further increased, only nanoparticles were deposited due to the strong collision between the ablated ZnO clusters and background gas. These ZnO nanostructured arrays had a preferred *c*-axis growth orientation on *c*-cut sapphire substrates. The room temperature PL spectrum shows strong intrinsic NBG UV emission peaks and rather weak defect-related visible emission proved their good crystal quality, especially for the ZnO nanowires. Due to their unique morphology characteristics, it was found that both the ZnO nanowalls and nanowires showed attractive field emission properties with low threshold field and big field enhancement factor.

Acknowledgments: The authors from China thank the supports from NSFC (51002065), Taishan Scholar Foundation, Shandong Provincial Science Foundation (BS2010CL003, ZR2010EL017), and UJN for new faculty. The work performed in Japan was supported by a Grant-in-Aid for Scientific Research from the Japan Society for the Promotion of Science (JSPS, 20360142) and Special Coordination Funds for Promoting Science and Technology from Japan Science and Technology Agency is also acknowledged. BC and HZ thank JSPS for fellowships.

References and Notes

1. H. B. Zeng, J. B. Zeng, B. Q. Cao, U. Gibson, Y. Bando, and D. Golberg, *Sci. Adv. Mater.* 2, 336 (**2010**).
2. H. B. Zeng, C. Y. Zhi, Z. H. Zhang, X. L. Wei, X. B. Wang, W. L. Guo, Y. Bando, and D. Golberg, *Nano Lett.* 10, 5049 (**2010**).
3. C. Czekalla, C. Sturm, R. Schmidt-Grund, B. Q. Cao, J. Z. Pérez, M. Lorenz, and M. Grundmann, *J. Vac. Sci. Technol. B* 27, 1780 (**2009**).
4. B. Q. Cao, M. Lorenz, M. Brandt, H. von Wenckstern, J. Lenzner, G. Biehne, and M. Grundmann, *Phys. Stat. Sol. (RRL)* 2, 37 (**2008**).
5. B. Q. Cao, W. P. Cai, G. T. Duan, Y. Li, Q. Zhao, and D. P. Yu, *Nanotechnology* 16, 2567 (**2005**).
6. B. Q. Cao, W. P. Cai, Y. Li, F. Q. Sun, and L. D. Zhang, *Nanotechnology* 16, 1734 (**2005**).
7. Z. L. Wang, *Nano Today* 5, 540 (**2010**).
8. B. Q. Cao, K. Sakai, D. Nakamura, I. A. Palani, H. B. Gong, H. Y. Xu, M. Higashihata, and T. Okada, *J. Phys. Chem. C* 115, 1702 (**2011**).
9. C. X. Xu, X. W. Sun, Z. L. Dong, and M. B. Yu, *Appl. Phys. Lett.* 85, 3878 (**2004**).
10. J. Shi, S. Grutzik, and X. D. Wang, *ACS Nano* 3, 1594 (**2009**).
11. R. Eason (ed.), Pulsed Laser Deposition of Thin Films, Wiley, NJ (**2007**).
12. M. Lorenz, K. Ellmer, A. Klein, and B. Rech (eds.), Pulsed laser deposition of ZnO-based films, in Transparent conductive ZnO, Springer, Berlin (**2008**).
13. A. M. Morales and M. Lieber, *Science* 279, 208 (**1998**).
14. M. Yan, H. T. Zhang, E. J. Widjaja, and R. P. H. Chang, *J. Appl. Phys.* 94, 5240 (**2003**).
15. M. Lorenz, E. M. Kaidashev, A. Rahm, Th. Nobis, J. Lenzner, G. Wagner, D. Spemann, H. Hochmuth, and M. Grundmann, *Appl. Phys. Lett.* 86, 143113 (**2005**).
16. B. Q. Cao, T. Matsumoto, M. Matsumoto, M. Higashihata, D. Nakamura, and T. Okada, *J. Phys. Chem. C* 113, 10975 (**2009**).

17. A. Rahm, G. W. Yang, M. Lorenz, T. Nobis, J. Lenzner, G. Wagner, and M. Grundmann, *Thin Solid Films* 486, 191 (**2005**).
18. R. Q. Guo, J. Nishimura, M. Ueda, M. Higashihata, D. Nakamura, and T. Okada, *Appl. Phys. A* 89, 141 (**2007**).
19. M. Kawakami, A. B. Hartanto, Y. Nakata, and T. Okada, *Jpn. J. Appl. Phys.* 42 L33 (**2003**).
20. T. Okada, B. H. Agung, and Y. Nakata, *Appl. Phys. A* 79, 1417 (**2004**).
21. S. Y. Li, C. Y. Lee, and T. Y. Tseng, *J. Cryst. Grow.* 247, 357 (**2003**).
22. B. Q. Cao, W. P. Cai, H. B Zeng, and G. T. Duan, *J. App. Phys.* 99, 073516 (**2006**).
23. H. B. Zeng, G. T. Duan, Y. Li, S. K. Yang, X. X. Xu, and W. P. Cai, *Adv. Funct. Mater.* 20, 561 (**2010**).
24. Y. K. Tseng, C. J. Huang, H. M. Cheng, I. N. Lin, K. S. Liu, and I. C. Chen, *Adv. Funct. Mater.* 13, 811 (**2003**).
25. N. G. Shang, F. Y. Meng, F. C. K. Au, Q. Li, C. S. Lee, I. Bello, and S. T. Lee, *Adv. Mater.* 14, 1308 (**2002**).
26. R. H. Fowler and L. W. Nordheim, *Proc. R. Soc. A* 119, 173 (**1928**).
27. J. H. Choy, E. S. Jang, J. H. Won, J. H. Chung, D. J. Jang, and Y. W. Kim, *Adv. Mater.* 15, 1911 (**2003**).
28. H. J. Fan, F. Bertram, A. Dadgar, J. Christen, A. Krost, and M. Zacharias, *Nanotechnology* 15, 1401 (**2004**).
29. H. B. Zeng, X. J. Xu, Y. Bando, U. K. Gautam, T. Y. Zhai, X. S. Fang, B. D. Liu, and D. Golberg, *Adv. Funct. Mater.* 19 3165 (**2009**).